$U^{BF}(5)$ to $SU^{BF}(3)$ shape phase transition in odd nuclei for $j = 1/2, 3/2$, and $5/2$ orbits: The role of the odd particle at the critical point

C. E. Alonso,[1] J. M. Arias,[1] L. Fortunato,[2] and A. Vitturi[2]

[1]*Departamento de Física Atómica, Molecular y Nuclear, Facultad de Física Universidad de Sevilla, Apartado 1065, E-41080 Sevilla, Spain*

[2]*Dipartimento di Fisica Galileo Galilei and INFN, Via Marzolo 8, I-35131 Padova, Italy*

(Received 10 November 2008; published 16 January 2009)

We investigate the phase transition in odd nuclei within the Interacting Boson Fermion Model in correspondence with the transition from spherical to stable axially deformed shape. The odd particle is assumed to be moving in the single-particle orbitals with angular momenta $j = 1/2,\ 3/2,\ 5/2$ with a boson-fermion Hamiltonian that leads to the occurrence of the $SU^{BF}(3)$ boson-fermion symmetry when the boson part approaches the SU(3) condition. Both energy spectra and electromagnetic transitions show characteristic patterns similar to those displayed by the even nuclei at the corresponding critical point. The role of the additional particle in characterizing the properties of the critical points in finite quantal systems is investigated by resorting to the formalism based on the intrinsic frame.

DOI: 10.1103/PhysRevC.79.014306 PACS number(s): 21.60.Fw, 21.60.Ev, 21.10.Re

I. INTRODUCTION

The study of shape phase transitions in finite nuclear quantal systems has recently been the subject of many investigations. Most of the work has been carried out for even-even nuclei, using either the Bohr Hamiltonian and the surface collective variables or algebraic approaches based on the use of interacting bosons. Recent review articles with references to the original works can be found in Refs. [1–4]. In the case of odd-even nuclei, where an odd particle is coupled to an even core undergoing a phase transition, attention has been put on the shape transition from sphericity to deformed γ-instability. In correspondence with the critical point in the even core, characterized by the critical point symmetry E(5) [5], two new boson-fermion critical point symmetries have been proposed, in the case of an odd particle moving in a single $j = 3/2$ shell (E(5/4) symmetry [6]) or in the $j = 1/2,\ 3/2,\ 5/2$ shells (E(5/12) symmetry [7]). Characteristic sequences of levels and ratios of electromagnetic transitions are predicted in both cases. Shape phase transitions in odd-even nuclei have been studied in Ref. [8] using a supersymmetric approach.

In this article we consider another leg of the Casten shape triangle, namely, the transition from the spherical vibrational behavior to stable axial deformation. This transition in the even-even case is normally named after the critical point symmetry X(5) [9] developed within the collective Bohr Hamiltonian formalism. The same situation has been studied within the Interacting Boson Model (IBM) by Rosensteel and Rowe [10]. In this work, we concentrate on the odd-even nuclei and couple along the transition the even-even core to an odd particle moving in the $j = 1/2,\ 3/2,\ 5/2$ single-particle shells. This situation is described within the framework of the IBFM (Interacting Boson Fermion Model), choosing a boson-fermion Hamiltonian that leads to the occurrence of the $SU^{BF}(3)$ boson-fermion symmetry when the boson part approaches the SU(3) condition. A previous study of shape phase transitions in odd-even nuclei using a supersymmetric approach was presented in Ref. [8].

The aim of this article is twofold. First we would like to identify other signatures of the phase transition, besides energies and electromagnetic transitions characterizing the X(5) situation in the even nuclei. We have shown that, for example, two-particle transfer matrix elements display characteristic behaviors and sudden changes in correspondence of the critical point [11], but we expect also that spectra and transitions in the neighbor odd nuclei should display characteristic features at the phase transition. Our second objective deals instead with the concept itself of critical point in finite quantal systems. For well-deformed cases, far from the critical point, we know that the contribution of the coupling to the additional odd particle (of the order of $1/N$) will not change appreciably the position of the sharp minimum in the deformation parameter for the energy surface. At the critical point, however, the energy surface in the even core is known to be rather flat in the deformation parameter, a feature that precisely characterizes the transition point. This behavior may imply that some of the energy surfaces characterizing the different states of the odd-even nucleus may be driven by the coupling in either direction (i.e., toward deformation or sphericity), effectively changing the position of the critical point.

The article is structured as follows. In Sec. II, the model Hamiltonian is presented and calculations along the transition region are performed in the laboratory frame. In Sec. III, the description of the transition region in the intrinsic frame is discussed. Section IV is devoted to studying in detail the critical point. Finally, a brief summary and some conclusions are given in Sec. V.

II. THE INTERACTING BOSON FERMION MODEL 1 (IBFM-1) ALONG THE U(5)-SU(3) LINE WITH COUPLING TO A $j = 1/2,\ 3/2,\ 5/2$ PARTICLE

We consider the spherical to axially deformed shape transition in the framework of the IBFM-1, when the odd particle occupies $j = 1/2, 3/2$, and $5/2$ orbitals. For this purpose we have chosen a Hamiltonian based on the one

used for the corresponding U(5) to SU(3) transition in the IBM-1 [10],

$$H^B = (1-x)n_d - \frac{x}{4N_B} Q_B \cdot Q_B, \qquad (2.1)$$

where N_B is the total boson number, n_d is the d-boson number operator, and $Q_B = (s^\dagger \times \tilde{d})^{(2)} + (d^\dagger \times \tilde{s})^{(2)} - \frac{\sqrt{7}}{2}(d^\dagger \times \tilde{d})^{(2)}$ is the boson quadrupole operator. The Hamiltonian H^B can be written in terms of the boson Casimir operators (the subindex 1 indicates linear while the subindex 2 stands for quadratic Casimir operators) as

$$H^B = (1-x)\mathcal{C}_1(U^B 5) - \frac{x}{8N_B}\left[\frac{3}{2}\mathcal{C}_2(\mathrm{SU}^B 3) - \frac{3}{8}\mathcal{C}_2(\mathrm{O}^B 3)\right]. \qquad (2.2)$$

In this work the definitions for the Casimir operators are those given in Ref. [12]. Because Casimir operators are defined up to a constant, some references may use different expressions for them (see Refs. [10] and [13]). We will use a similar form for the Hamiltonian that describes the transition from spherical to axially deformed odd-even nuclei within the IBFM-1,

$$H^{BF} = (1-x)\mathcal{C}_1(\mathrm{U}^{BF} 5) - \frac{x}{8N_B}\left[\frac{3}{2}\mathcal{C}_2(\mathrm{SU}^{BF} 3) - \frac{3}{8}\mathcal{C}_2(O^{BF} 3)\right], \qquad (2.3)$$

where the superindex BF stands for boson-fermion. The Bose-Fermi Casimir operators used in this work are defined as given in Ref. [14].

To get physical insight into the problem, we rewrite the boson-fermion Hamiltonian (2.3) as

$$H^{BF} = (1-x)(n_d + n_{\frac{3}{2}} + n_{\frac{5}{2}}) - \frac{x}{4N_B} Q_{BF} \cdot Q_{BF}, \qquad (2.4)$$

where $n_{\frac{3}{2}}(n_{\frac{5}{2}})$ is the $j = 3/2(5/2)$ fermion number operator and $Q_{BF} = Q_B + q_F$ is the total (boson-fermion) quadrupole operator. The explicit expression for the fermion quadrupole operator q_F can be obtained from Eq. (3.5) of Ref. [13] for $n = 2$ and $\ell, \ell' = 0, 2$,

$$q_F = -\sqrt{\frac{4}{5}}[(a^+_{1/2}\tilde{a}_{3/2})^{(2)} - (a^+_{3/2}\tilde{a}_{1/2})^{(2)}] - \sqrt{\frac{6}{5}}[(a^+_{1/2}\tilde{a}_{5/2})^{(2)} + (a^+_{5/2}\tilde{a}_{1/2})^{(2)}] - \frac{\sqrt{7}}{2}\left\{-\sqrt{\frac{14}{25}}(a^+_{3/2}\tilde{a}_{3/2})^{(2)} + \sqrt{\frac{6}{25}} \times [(a^+_{3/2}\tilde{a}_{5/2})^{(2)} - (a^+_{5/2}\tilde{a}_{3/2})^{(2)}] - \sqrt{\frac{24}{25}}(a^+_{5/2}\tilde{a}_{5/2})^{(2)}\right\}. \qquad (2.5)$$

Note that the choice of the fermion space is such that one can profitably visualize the three angular momenta as arising from the coupling of a pseudo spin 1/2 with a pseudo orbital angular momentum 0 or 2. Because the Hamiltonian does not depend on the pseudo spin, this gives rise to repeated level couplets with $J = L \pm 1/2$ (when $L \neq 0$). This degeneracy might eventually be broken by introducing a term proportional to J^2 in the Hamiltonian.

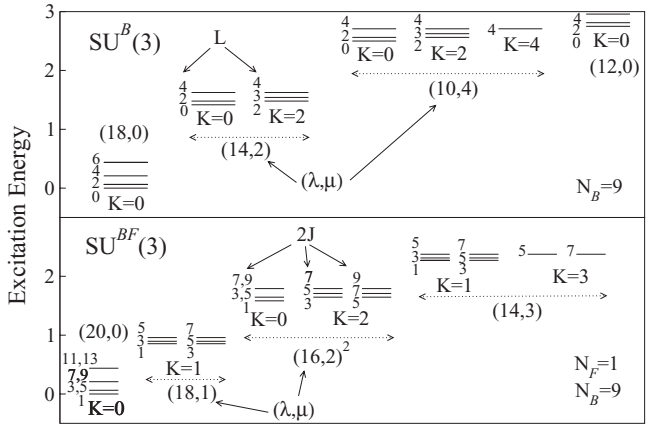

FIG. 1. Spectra obtained in the $\mathrm{SU}^B(3)$ (upper panel) and $\mathrm{SU}^{BF}(3)$ limits (lower panel) for $N_B = 9$ bosons. In the lower panel the horizontal lines in the $K = 0$ bands represent two states (except for $L = 0$).

With our choice of the Hamiltonian (2.4) we obtain for $x = 0$ the $\mathrm{U}^{BF}(5)$ dynamic symmetry and for $x = 1$ the $\mathrm{SU}^{BF}(3)$ one. In the lower part of Fig. 1 we show some of the levels obtained in the latter case assuming that the core is made up of $N_B = 9$ bosons to which a single fermion ($N_F = 1$) is coupled. For a comparison, in the upper part the corresponding spectrum for the even-even nucleus, $N_B = 9$, is shown. In the odd system, N_B bosons plus one fermion, the levels are arranged in rotational bands, characterized by the quantum numbers (λ, μ) K and $2J$. Some of them can be identified with those of the even core, in the upper panel, with N_B bosons (in this case the levels are labeled by L), but others [not fully symmetric with μ odd, e.g., the $(\lambda = 18, \mu = 1)$] arise genuinely from the fermion-boson nature of the problem. Note that in each rotational band the energy goes as $L(L+1)$ and not as $J(J+1)$. In addition to the degeneracy coming from the pseudo spin coupling, we have degeneracies coming from the bosonic plus fermionic orbital parts.

Some of the degeneracies disappear as one moves away from the $\mathrm{SU}^{BF}(3)$ limit by acting on the control parameter x. The transition from $\mathrm{SU}^{BF}(3)$ toward $\mathrm{U}^{BF}(5)$ is more complicated than the one studied before [15] from $\mathrm{O}^{BF}(6)$ to $\mathrm{U}^{BF}(5)$. In that case there was a common subgroup, $\mathrm{O}^{BF}(5)$, which supplied labels all over the transition. This is no longer the case, and we can only use "asymptotic" $\mathrm{SU}^{BF}(3)$ quantum numbers (λ, μ) to label the states outside the extremes of the transition. The possibility of using as asymptotic quantum numbers the ones of $\mathrm{U}^{BF}(5)$ is a worse choice because there are more degeneracies at this extreme of the transition. One could invoke the concept of quasi dynamical symmetry to have a criterion on how to assign the asymptotic quantum numbers. Similarly the arrangement of the levels into bands is not always univoque and the information from the electromagnetic matrix elements may not always be sufficient.

In Fig. 2 we show the full evolution of the energy of some selected levels, normalized to the energy of the first excited state, along the transition, still in the case of $N_B = 9$. The states are labeled all over with the SU(3) quantum numbers (λ, μ), which are strictly valid only for $x = 1$, and L. For each

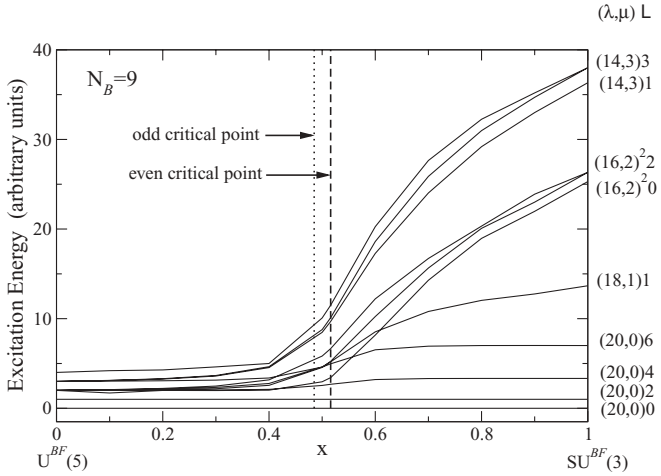

FIG. 2. Energy levels (normalized to the excitation energy of the first excited state) as a function of the control parameter $\dot{x}$ in the Hamiltonian (2.3). A number, $N_B = 9$, of bosons has been assumed. Each state is characterized by the (λ, μ) asymptotic quantum numbers (strictly valid only for $x = 1$, at the SU^{BF}(3) extreme) and L. The two vertical lines indicate the position of the critical value of x for the even-even and odd-even systems.

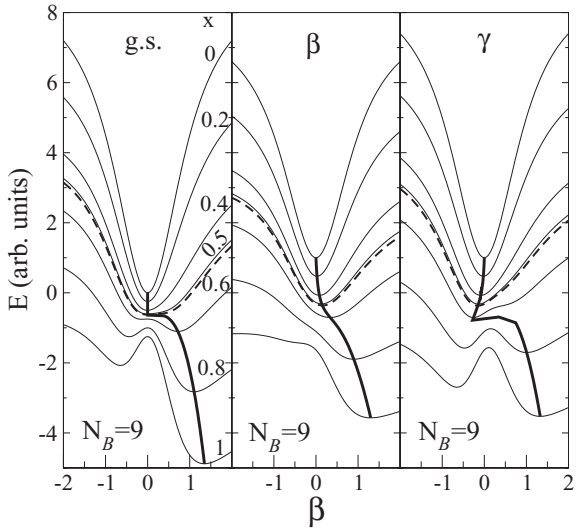

FIG. 3. Energy surfaces for even-even nuclei with $N_B = 9$ as a function of the deformation, β, for different values of the control parameter x and for different bands: ground state band (left panel), β band (central panel), and γ band (right panel). The curves at the critical value are shown as dashed. The position of the minima are connected by a bold solid line. The calculations are performed for $\gamma = 0$.

level the total angular momenta come from the coupling of the O^{BF}(3) quantum number L to the SU$_s^F$(2) quantum number S. In general the states are doubly degenerate except for $L = 0$. The general behavior of the energy levels is rather smooth close to the dynamic symmetry limits, changing more rapidly in the neighborhood of the critical point for the even-even core, indicated by a dashed vertical line. It is clear from the figure that by using only energies (and eventually transition rates) it is rather difficult to single out the precise position of the critical point in the absence of other signatures, due to the finite number of particles. The key way is based on the concepts of intrinsic frame and energy surfaces, as is shown in the next section.

III. THE INTRINSIC FRAME DESCRIPTION AND THE CRITICAL POINT

A useful way of looking at phase transitions is to resort to the concept of intrinsic states and associated energy surfaces. In the case of the Interacting Boson Model for even-even nuclei one introduces a ground band intrinsic state of the form

$$\Phi_{\rm gs}(\beta, \gamma) = \frac{1}{\sqrt{N_B!}}[b^\dagger_{\rm gs}(\beta, \gamma)]^{N_B}|0\rangle, \tag{3.1}$$

where $|0\rangle$ is the boson vacuum. The basic quadrupole boson is given in the form

$$b^\dagger_{\rm gs}(\beta, \gamma) = \frac{1}{\sqrt{1+\beta^2}}\left[s^\dagger + \beta\cos\gamma d^\dagger_0 + \frac{\beta}{\sqrt{2}}\sin\gamma(d^\dagger_2 + d^\dagger_{-2})\right], \tag{3.2}$$

and β and γ play a role similar to the intrinsic collective variables in the Bohr Hamiltonian. The ground state energy surface is obtained as the expectation value of the boson Hamiltonian (2.1) in the intrinsic state, i.e.,

$$E_{\rm gs}(\beta, \gamma) = \langle\Phi_{\rm gs}(\beta, \gamma)|H^B|\Phi_{\rm gs}(\beta, \gamma)\rangle. \tag{3.3}$$

In our specific case, for any value of the control parameter x the energy surface has a minimum, as a function of the parameter γ, for $\gamma = 0$. In other words, our boson Hamiltonian can never lead to a stable triaxial shape. As far as the β dependence is concerned, we show in Fig. 3 (left panel) the ground state energy surfaces for different values of the control parameter x. The figure shows in a clear way the occurrence of the critical point. For small values of x the system finds more convenient a spherical shape ($\beta_{\rm min} = 0$), while after the critical value a deformed minimum becomes lower in energy. The occurrence of this first-order transition is shown in the figure by a bold solid line that singles out the position of the minima for the different values of x. As is well known, precisely at the critical point the energy surface is rather flat [9]. The phase transition occurs for a value of the control parameter $x = 16N_B/(34N_B - 27)$. In our case with $N_B = 9$ bosons, the critical value $x_c \simeq 0.516$ is obtained, rather close to the asymptotic value $x \simeq 0.47$ valid for large values of N_B.

The situation may be modified if one looks at excited states. We are, in fact, dealing with a finite quantal system, and one knows that one-phonon excitations are expected to produce energy corrections of the order of $1/N_B$. This can be important precisely at the critical point where the energy surface is flat and small corrections can drive the system in either direction (i.e., toward deformation or sphericity). In the central and right panels of Fig. 3 we show the energy surfaces associated with the β and γ bands. The corresponding intrinsic states are given

by

$$\Phi_\beta(\beta,\gamma) = \frac{1}{\sqrt{(N_B-1)!}}[b^\dagger_{\rm gs}(\beta,\gamma)]^{N_B-1}b^\dagger_\beta(\beta,\gamma)|0\rangle,$$
$$\Phi_\gamma(\beta,\gamma) = \frac{1}{\sqrt{(N_B-1)!}}[b^\dagger_{\rm gs}(\beta,\gamma)]^{N_B-1}b^\dagger_\gamma(\beta,\gamma)|0\rangle, \quad (3.4)$$

where the basic β and γ bosons are given by

$$b^\dagger_\beta(\beta,\gamma) = \frac{1}{\sqrt{1+\beta^2}}\left[-\beta s^\dagger + \cos\gamma d^\dagger_0 + \right.$$
$$\left. + \frac{1}{\sqrt{2}}\sin\gamma(d^\dagger_2 + d^\dagger_{-2})\right] \quad (3.5)$$

and

$$b^\dagger_\gamma(\beta,\gamma) = \frac{1}{\sqrt{2}}(d^\dagger_2 - d^\dagger_{-2}). \quad (3.6)$$

One can see from the figure that, *ceteris paribus* (that is, all other things being the same), the β band tends to favor prolate deformation, while the γ band for small values of x drives the system slightly on the opposite direction (toward oblate deformation). This has no significant effect for well-deformed systems, but if one compares the three energy surfaces at the ground-state critical value (dashed curves in the three frames), at variance to the flat surface for the ground state, we have prolate and oblate minima for the β and γ bands, respectively. As a result, the effective critical point is shifted to higher values of x for the γ band, with the opposite tendency for the β band.

This discussion on the critical point for excited states in boson systems anticipates a similar behavior for the coupled boson-fermion systems in odd nuclei. The reader is referred to Ref. [16] for a recent account of the topic of phase transitions in excited states. Intrinsic frame states for odd systems can be constructed by coupling the odd single-particle states (with each angular momentum j and magnetic component k) to the intrinsic states of the even core. The lowest states of the odd nucleus are expected to originate from the coupling to the intrinsic ground-state $\Phi_{\rm gs}(\beta,\gamma)$. One first constructs the coupled states

$$\Psi_{jk}(\beta,\gamma) = \Phi_{\rm gs}(\beta,\gamma)\otimes|jk\rangle \quad (3.7)$$

and diagonalize in this basis (for each value of β and γ) the total boson-fermion Hamiltonian, giving a set of energy eigenvalues $E_n(\beta,\gamma)$, n being a running index to count the solutions. In our specific $U^F(12)$ algebra we have a total of 12 components, but this is restricted to 6 within the symmetry $k \leftrightarrow -k$. In addition, because the Hamiltonian does not depend on the pseudo spin, the active role is played by the pseudo orbital angular momenta $l = 0$ (with $k_l = 0$) and $l = 2$ (with $k_l = 0, \pm1, \pm2$). We expect, therefore, for the general Hamiltonian (2.4) four different intrinsic states and consequently four different bands. For $\gamma = 0$ the Hamiltonian preserves the quantum number k and the diagonalization is independently done for each value of k. In this case we obtain two states with $k = 1/2$, one degenerate pair with $k = 1/2, 3/2$ and the last degenerate with $k = 3/2,\ 5/2$.

We first show in Fig. 4 (left panel) the boson-fermion energy surfaces for a well-deformed case ($x = 1$, leading to the $SU^{BF}(3)$ dynamical symmetry) as a function of the deformation parameter β. A value $\gamma = 0$ is assumed. For a better comparison we also include, as a dashed line, the energy surface corresponding to the even–even core ground state. A number, $N_B = 9$, of bosons has been assumed for the core. We can see that all energy surfaces display the minimum for the same value of the deformation parameter β. In this well-deformed case, therefore, the addition of the extra particle is not changing the features of the system. Each state of the odd nucleus can be put in correspondence with one of the rotational bands appearing in Fig. 1. The lowest $k = 1/2$ state is the intrinsic state of the ground band (20,0) of Fig. 1. Similarly the next $k = 1/2,\ 3/2$ state is the intrinsic state of the doubly degenerate band (18,1). Finally the last $k = 1/2$ and $k = 3/2,\ 5/2$ states are the band heads of one of the two degenerate multiple bands with quantum numbers (16,2). Note that the intrinsic frame approach reproduces quite well the energies of the band heads. We get, from the energies of the minima, excitation energies equal to 0.750, 1.51, and 1.51, very close to the values 0.854, 1.58, and 1.65 obtained in the laboratory frame.

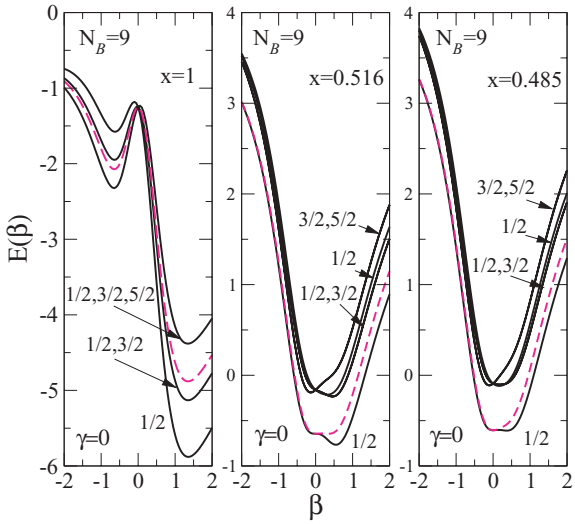

FIG. 4. (Color online) Energy surfaces in the odd-even nucleus with $N_B = 9$ as a function of the deformation parameter β. The different curves refer to the different intrinsic states. The dashed lines give the corresponding energy surfaces for the even-even case. The three panels correspond to different choices of the control parameter x. The left panel ($x = 1$) corresponds to the $SU^{BF}(3)$ dynamical symmetry; the other panels correspond to the critical points in the even-even case ($x = 0.516$) and the odd-even case ($x = 0.485$). In all cases we have assumed $\gamma = 0$, so that states are characterized by good k values.

The situation is different around the critical point of the even-even core (central frame). We see from the figure that in this case the odd particle drives the system toward deformation or sphericity (according to the different states of the odd-even nucleus). This gives rise to an effective shift of the critical point. For example, for the ground band, the critical point moves to $x = 0.485$, where in fact the corresponding energy surface becomes flat (right panel).

We conclude this section with some remarks on the γ dependence. In Fig. 5 we show the ground-state energy

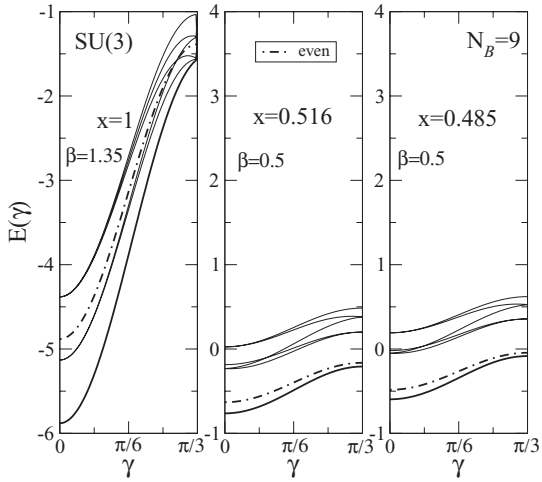

FIG. 5. Ground-state energy surfaces as a function of γ for the even-even (dot-dashed) and odd-even cases (lowest solid line). The same three cases as in Fig. 4 are taken for the control parameter x. In each case β is close to the value corresponding to the minimum of the energy surface in the odd-even nucleus. Higher thin solid lines give the energy surfaces of excited states as a function of γ for the odd-even case.

surfaces for the even-even (dot-dashed) and odd-even case (solid) as a function of γ for $x = 1$, $x = 0.516$ (critical point for the even-even nucleus), and $x = 0.485$ (critical point for the odd-even nucleus) and selected values of β around the minima of the ground-state energy surfaces. As we mentioned before, the energy surfaces for our boson Hamiltonian as a function of γ display minima for $\gamma = 0$ for all values of the control parameter x. The depth of the minima changes along the transition. These behaviors are also observed for the boson-fermion Hamiltonian. We see in Fig. 5 that, while for the well-deformed case (left panel) the minimum at $\gamma = 0$ is very deep, the minimum at the critical point (either for the even-even nuclei or the odd-even nuclei) is rather shallow and the system tends to be more γ soft.

IV. SPECTRA AND TRANSITIONS AT THE CRITICAL POINT

We calculate the odd-even nucleus spectrum for $x_{c-oe} = 0.485$, according to the Hamiltonian (2.4). The resulting sequence of levels, arranged in bands, is shown in the lower panel in Fig. 6. For a better comparison, in the upper panel of the figure we show the corresponding spectrum for the even-even core at its critical point. Degeneracies coming from the bosonic plus fermionic orbital parts are broken. In addition, in the odd-even spectrum, in some bands with odd μ the order of the J's has been altered.

Comparing the even-even and odd-even spectra, energies ratios for equivalent states (those that have (λ, μ) in the even-even and $(\lambda + 2, \mu)$ in the odd-even) differ slightly. To be more quantitative, in Table I we present a comparison of some selected energy ratios. The values of these ratios for the critical odd-even and even-even nuclei are quite close to each other, but rather different from the X(5) values, especially the $\frac{E_{0_2^+} - E_{0_1^+}}{E_{2_1^+} - E_{0_1^+}}$

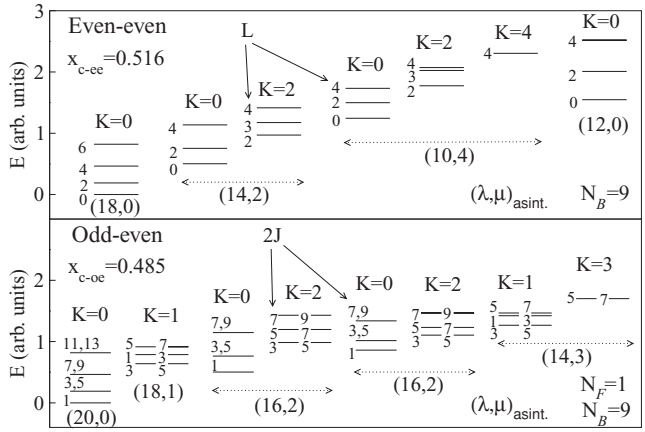

FIG. 6. Spectra obtained at the critical points in the case of $N_B = 9$. The upper panel displays the spectrum in the even-even case ($x_c = 0.516$), the lower panel displays the spectrum in the neighbor odd-even, boson-fermion case ($x_c = 0.485$).

ratio, as expected. The energy ratios within the ground-state band provided by the X(5) values are closer to those of SU(3) than those obtained within IBM for the studied critical points.

Additional important information comes from the electromagnetic transitions. The corresponding intensities for selected transitions are reported in Fig. 7. Also in this case the general behavior for the odd-even case follows closely the one for the even-even case. It can be observed that, although (λ, μ) are not good quantum numbers for $x = x_{c-oe}$, transitions in the odd-even nucleus between different $(\lambda, \mu)_{asint}$ are highly hindered. In Table I few selected $B(E2)$ ratios are presented for the even-even and the odd-even nuclei at the critical points. The X(5) results for the even-even case are also presented

TABLE I. Selected energy and reduced matrix element ratios at the critical point of the even-even ($x_c = 0.516$) and odd-even ($x_c = 0.485$) nucleus for $N_B = 9$. In the second, third, and fourth columns the corresponding U(5), SU(3), and X(5) results for the even-even nucleus are given as references. The ratios given in the first column correspond to the even-even nucleus, and the corresponding ratios for the odd-even nucleus are given in the last column. The SU(3) value marked with $*$ depends on the parameters used in the SU(3) Hamiltonian; the value written in this table corresponds to the Hamiltonian (2.1) with $x = 1$ and $N_B = 9$.

	Even-even				Odd-even	
Ratio	U(5)	SU(3)	X(5)	IBM	IBFM	Ratio
$\frac{E_{4_1^+} - E_{0_1^+}}{E_{2_1^+} - E_{0_1^+}}$	2.00	3.33	2.91	2.45	2.44	$\frac{E_{9/2_1^+} - E_{1/2_1^+}}{E_{5/2_1^+} - E_{1/2_1^+}}$
$\frac{E_{6_1^+} - E_{0_1^+}}{E_{2_1^+} - E_{0_1^+}}$	3.00	7.00	5.45	4.33	4.29	$\frac{E_{13/2_1^+} - E_{1/2_1^+}}{E_{5/2_1^+} - E_{1/2_1^+}}$
$\frac{E_{0_2^+} - E_{0_1^+}}{E_{2_1^+} - E_{0_1^+}}$	2.00	22.67*	5.67	2.65	2.64	$\frac{E_{1/2_2^+} - E_{1/2_1^+}}{E_{5/2_1^+} - E_{1/2_1^+}}$
$\frac{B(E2;4_1^+ \to 2_1^+)}{B(E2;2_1^+ \to 0_1^+)}$	2.00	1.43	1.58	1.71	1.73	$\frac{B(E2;9/2_1^+ \to 5/2_1^+)}{B(E2;5/2_1^+ \to 1/2_1^+)}$
$\frac{B(E2;6_1^+ \to 4_1^+)}{B(E2;2_1^+ \to 0_1^+)}$	3.00	1.57	1.96	2.00	2.06	$\frac{B(E2;13/2_1^+ \to 9/2_1^+)}{B(E2;5/2_1^+ \to 1/2_1^+)}$
$\frac{B(E2;2_1^+ \to 0_2^+)}{B(E2;2_1^+ \to 0_1^+)}$	1.20	0.00	0.13	0.24	0.25	$\frac{B(E2;5/2_1^+ \to 1/2_2^+)}{B(E2;5/2_1^+ \to 1/2_1^+)}$

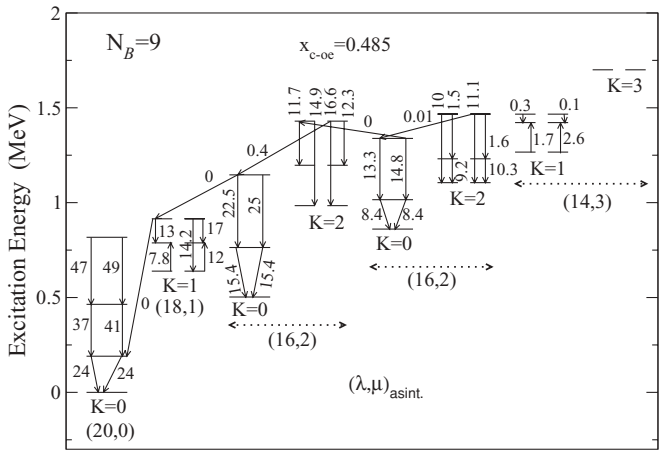

FIG. 7. Reduced $E2$ transition probabilities for $x = x_{c-oe}$ and $N_B = 9$. For $K = 0$ bands, in levels with $L \neq 0$ (see the lower panel of Fig. 6 to know the J of each level), the left (right) arrow represents the transition from the initial state $J_i = L_i - 1/2 (J_i = L_i + 1/2)$ to the final state $J_f = L_f - 1/2 (J_f = L_f + 1/2)$. For $K \neq 0$ the left (right) horizontal line represents states with the lowest (highest) J for the corresponding L as represented in the lower panel of Fig. 6.

as reference. It is clear that the odd-even results follow closely the even-even ones. Major differences with the X(5) results are found in transitions involving the 0_2^+ state. The similarity between the even-even and odd-even systems is easily understood in the limit of pure states. Assuming

$$|1/2_1\rangle \approx |L_B = 0_1 \times j = 1/2\rangle$$
$$|1/2_2\rangle \approx |L_B = 0_2 \times j = 1/2\rangle$$
$$|5/2_1\rangle \approx |L_B = 2_1 \times j = 1/2\rangle,$$

all the $B(E2)$ ratios shown in Table I have to be equal in the even-even nucleus and in the corresponding transition in the odd-even system. This is clearly the situation observed in Table I although in the calculations leading to Table I states in the odd-even nucleus are not pure but have other small components.

V. SUMMARY AND CONCLUSIONS

In this article we have considered, within the IBFM, the case of the coupling of an odd particle moving in the $j = 1/2, 3/2$, and $5/2$ orbitals to a boson core undergoing a transition from U(5) to SU(3). We have followed the evolution of the spectrum along the transition and studied in detail energies and transitions in correspondence with the critical point. The position of the critical point has been discussed by resorting to the intrinsic fermion-boson states. We found that the position of the critical point has been shifted by the addition of the odd particle with respect to the even case, but the magnitude of this shift is of the order of $1/N$, N being the number of active bosons. As a consequence the behavior of the odd and even systems at the corresponding critical points are rather similar, with the exclusion of the additional bands in the odd case that only arise from the fermion-boson character of the system. Our study confirms the importance of the odd nuclei as necessary signatures to characterize the occurrence of the phase transition and to determine the precise position of the critical point.

ACKNOWLEDGMENTS

This work has been partially supported by the Italian-Spanish INFN-MCYT Agreement, by the Spanish Ministerio de Educación y Ciencia and the European Regional Development Fund (FEDER) under Project FIS2008-04189, by the Spanish Consolider-Ingenio 2010 Programme CPAN (CSD2007-00042), and by Junta de Andalucía under Projects FQM160 and P07-FQM-02894.

[1] L. Fortunato, Eur. Phys. J. A **26**, s01, 1 (2005).
[2] R. F. Casten, Nature Physics **2**, 811 (2006).
[3] R. F. Casten and E. A. McCutchan, J. Phys. G: Nucl. Part. Phys. **34**, R243 (2007).
[4] P. Cejnar and J. Jolie, Prog. Part. Nucl. Phys. **62**, 210 (2009).
[5] F. Iachello, Phys. Rev. Lett. **85**, 3580 (2000).
[6] F. Iachello, Phys. Rev. Lett. **95**, 052503 (2005).
[7] C. E. Alonso, J. M. Arias, and A. Vitturi, Phys. Rev. Lett. **98**, 052501 (2007).
[8] J. Jolie, S. Heinze, P. Van Isacker, and R. F. Casten, Phys. Rev. C **70**, 011305(R) (2004).
[9] F. Iachello, Phys. Rev. Lett. **87**, 052502 (2001).
[10] G. Rosensteel and D. J. Rowe, Nucl. Phys. **A759**, 92 (2005).
[11] R. Fossion, C. E. Alonso, J. M. Arias, L. Fortunato, and A. Vitturi, Phys. Rev. C **76**, 014316 (2007).
[12] F. Iachello and A. Arima, *The Interacting Boson Model* (Cambridge University Press, Cambridge, UK, 1987).
[13] R. Bijker and V. K. B. Kota, Ann. Phys. **187**, 148 (1988).
[14] F. Iachello and P. Van Isacker, *The Interacting Boson Fermion Model* (Cambridge University Press, Cambridge, UK, 1991).
[15] C. E. Alonso, J. M. Arias, and A. Vitturi, Phys. Rev. C **75**, 064316 (2007).
[16] M. A. Caprio, P. Cejnar, and F. Iachello, Ann. Phys. **323**, 1106 (2008).